Dynamics of the interaction of O_2 with stepped and damaged Ag surfaces

2002 J. Phys.: Condens. Matter 14 6065

(http://iopscience.iop.org/0953-8984/14/24/310)

INSTITUTE OF PHYSICS PUBLISHING JOURNAL OF PHYSICS: CONDENSED MATTER

J. Phys.: Condens. Matter **14** (2002) 6065–6079 PII: S0953-8984(02)34779-9

Dynamics of the interaction of O_2 with stepped and damaged Ag surfaces

L Savio, L Vattuone and M Rocca[1]

IMEM-CNR and Istituto Nazionale di Fisica della Materia, Dipartimento di Fisica, Via Dodecaneso 33, 16146 Genova, Italy

E-mail: rocca@fisica.unige.it

Received 12 March 2002
Published 31 May 2002
Online at stacks.iop.org/JPhysCM/14/6065

Abstract

The role of defects in catalytic reactions, especially those involving low rates and high degrees of selectivity, has been debated ever since the very early days of surface science. However, most studies on gas–surface interaction and chemisorption performed under controlled laboratory conditions have dealt so far with nearly perfect low-Miller-index surfaces, which are rather unlike the active powders employed as catalysts in industrial reactors. The failure in reproducing some chemical reactions, which occur readily under industrial conditions, was therefore often ascribed to the so-called structure gap separating the surface science approach from the real industrial conditions. Overcoming this limit without losing control over the experiment at the nanoscopic scale is therefore an issue of pivotal importance. It can be attacked by studying adsorption on either single-crystal surfaces damaged by ion bombardment or on surfaces aligned along high-Miller-index planes. In this paper we shall discuss O_2 interaction with Ag(410), a vicinal surface of Ag(100) characterized by open (110)-like steps and by (100) terraces. The use of a supersonic molecular beam to dose O_2 allowed us to gain information on the interaction of the gas-phase molecules with steps and terraces separately, by selecting the angle of incidence and the impact energy. The open steps turned out to be active sites for dissociation, while flat Ag(100) planes are unreactive. For molecular adsorption a reduction in the activation barrier is observed at the steps, while the Ag(100) nanoterraces are much less reactive than wide (100) planes. The main results are confirmed by the preliminary investigation of O_2/Ag(210).

1. Introduction

Industrial catalysts and gas sensors have been developed empirically by chemists and chemical engineers by trial-and-error procedures. In spite of the high levels of efficiency and selectivity

[1] Author to whom any correspondence should be addressed.

which can be reached, further improvement of the control on catalytic reactions is mandatory in several cases to reduce production costs and meet the more severe requirements imposed to limit the environmental impact of chemical processes. Physicists and chemical physicists have contributed to the advancement of this knowledge via the so-called 'surface science approach', which consists in analysing the sequence of elementary steps of chemical reactions and in identifying and characterizing the active sites and the mechanisms operating at the atomic level [1]. Adsorption, surface diffusion, chemical transformation, and desorption of the adsorbed species were therefore studied under controlled ultrahigh-vacuum conditions, using single-crystal surfaces and performing state-resolved experiments. The systems were simulated with numerical codes based on *ab initio* methods, reproducing the experimental results. The link between these idealized conditions and the industrial reactions is however not straightforward, as reactors are generally operated at high pressure and high temperature. Moreover, the catalyst's material is a highly dispersed state of small particles, i.e. quite unlike the nearly perfect low-Miller-index surfaces used by surface scientists. Such shortcomings of the surface science approach to catalysis are known as pressure and structure gaps, respectively. The ten-orders-of-magnitude difference in pressure may imply that the molecules populating the high-energy tail of the Boltzmann distribution dominate the reaction if the adsorption of one of the reactants is activated. The structure can, on the other hand, limit the reaction rate if one of the elementary steps of a reaction occurs only at a minority site associated with a surface defect.

The decisive role of defects was demonstrated recently for NO and N_2 adsorption on Ru(0001) [2–4], for which systems dissociation is observed at close-packed atomic steps but not at terraces. In other experiments, defects were introduced on purpose by damaging single-crystal surfaces by ion bombardment. Large effects were found for dissociative adsorption of NH_3 on Ru(0001) [5] and O_2 on Ag(100) [6,7]. Alternatively, the role of defects in adsorption processes was studied using single-crystal surfaces with a well defined majority defect. For O_2/Pt(533) the closed, (100)-like, steps were shown to be the active sites for the conversion from the physisorbed to the chemisorbed precursor [8]. This defect is therefore the determinant for the reactivity of Pt(111) planes. In other experiments it was shown by microcalorimetry that C_2H_4 adsorbs initially as quad-σ-acetylene and then, at higher coverage, as ethylidyne on Pt(211), while on the more corrugated Pt(311), only ethylidyne forms [9]. Studying vicinal surfaces is however meaningful only whenever indications of the nature of the active site are available from previous experiments.

The role of defects for the O_2/Ag interaction is particularly intriguing, since this system has been thoroughly investigated in the past, searching for the oxygen moiety active in the ethylene epoxidation reaction. This reaction occurs industrially only on Ag powders and shows a very high selectivity with respect to the competing channels of total combustion [10,11]. In spite of the research efforts, the active species has so far escaped identification. These studies showed that O_2 adsorption is structure sensitive [12,13], molecular chemisorption in the peroxide state being observed only for Ag(110) [14,15] and Ag(100) [16]. For adsorption on Ag(111), in contrast, a superoxide state was reported with a much lower sticking coefficient [17–19]. Such a state was however not observed in subsequent studies, which led to the conclusion that the (111) planes are inert [20,21]. Moreover, thermal dissociation occurs efficiently for Ag(110), while on Ag(100) it takes place only at defects, tentatively identified with kink sites [22]. On sputtered Ag(100), significant O_2 dissociation occurs also at $T = 100$ K. When the surface is organized in a checkerboard structure of square pits, as obtained by sputtering with the crystal close to room temperature (RT), the dissociation probability scales with nearly unitary ratio with the density of the kinks present at the corners of the pits [6,7]. Following these indications, we investigated the interaction of O_2 with stepped Ag(410) surfaces, characterized by (100)

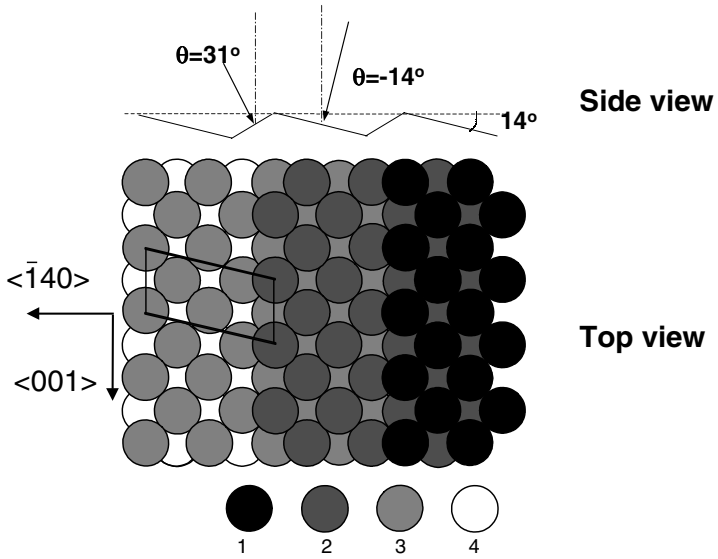

Figure 1. The geometry of the Ag(410) surface. The scattering plane is aligned along the $\langle\bar{1}, 4, 0\rangle$ direction (across the monatomic steps). The surface unit cell is also shown.

terraces and a high (25%) concentration of open steps running along the $\langle 001\rangle$ direction (i.e. having step heights with (110)-like geometry; see figure 1). We found that low-temperature dissociation does indeed also occur in this case and that, when the defect is exposed, the activation energy for molecular adsorption is considerably lower than that at terrace sites [23].

2. Experimental procedure

Experiments were performed in an ultrahigh-vacuum apparatus [24] which combines a supersonic molecular beam and a high-resolution electron energy-loss spectrometer (HREELS), as well as the usual facilities for preparing the surface *in situ* and controlling its cleanliness and order. The supersonic molecular beam allows dosing the O_2 molecules at a selected angle of incidence, θ, and at given translational energy, E_i. A quadrupole mass spectrometer (QMS), not in line of sight with the surface, is employed to measure the sticking coefficient with the retarded reflector method of King and Wells [25] (KW in the following). The adsorption products are vibrationally characterized by HREEL spectroscopy. The spectra were recorded specularly at 60° incidence and low incident electron energy, $E_e = 1.9$ eV, to enhance dipole scattering. Further information on the experimental set-up can be found in [24].

The stepped samples used in the experiments are 7 mm diameter Ag discs oriented, respectively, within 1° of the (410) plane and within 0.25° of the (210) plane. The flat (100) surface is in contrast a 10 mm diameter Ag disc oriented within 0.1° of the (100) plane. The (410) geometry is shown schematically in figure 1. It consists of three-atom-row large terraces with (100) symmetry and of steps oriented along the $\langle 001\rangle$ directions, showing therefore (110)-like nanofacets. The main angles, corresponding to trajectories hitting the surface normal to the terraces and normal to the step heights, are shown in the figure, too, and read $\theta = -14°$ and 31°, respectively. Ag(210) looks similar, but the (100)-like terraces are so small that no complete (100) unit cell is present. The surfaces are prepared *in situ* by sputtering and annealing

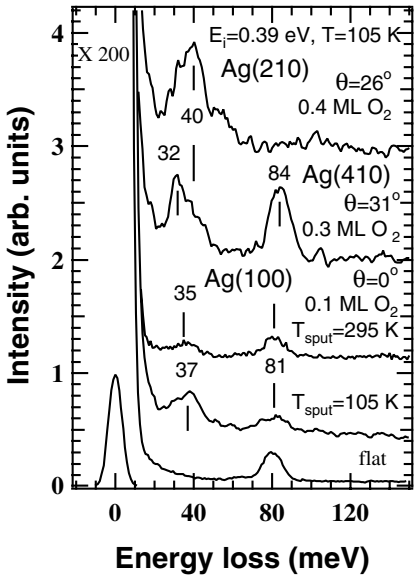

Figure 2. HREEL spectra recorded after dosing O_2 with $E_i = 0.39$ eV onto flat and sputtered Ag(100), Ag(410), and Ag(210) at $T = 105$ K. O_2 exposure is performed at normal incidence for Ag(100) and normal to the (110) step heights for the stepped surfaces. The losses in the 30–40 meV region are due to adatom surface vibrations; the losses at 80–84 meV are due to the internal stretch mode of O_2 admolecules. Only molecular adsorption takes place on flat Ag(100), while adatoms and admolecules coexist for sputtered Ag(100) and Ag(410). The final adsorption state is purely dissociative for Ag(210).

to a crystal temperature, T, of 700 K until good-quality patterns are observed by means of low-energy electron diffraction (LEED). The supersonic molecular beam was collimated to a spot diameter of 2 mm at the crystal for KW measurements and to a diameter larger than the sample for HREELS experiments. The translational energy, E_i, of the impinging molecules is controlled by varying the temperature of the ceramic nozzle and by seeding the gas in He (3% concentration of the reactant in most experiments). The energy resolution of the supersonic beam is $\pm 10\%$. The O_2 dose, $\chi = \phi t$, is deduced by measuring the exposure time, t, and the beam flux, ϕ. The latter is determined by a spinning rotor gauge and reads typically 0.079 ± 0.008 ML s^{-1} for the pure beam and 0.040 ± 0.005 ML s^{-1} for the seeded beam (1 ML $= 1.14 \times 10^{15}$ atoms cm^{-2}, the density of Ag(410)) when the nozzle is at RT.

3. Data presentation

In figure 2 we compare the HREEL spectra recorded after exposing Ag surfaces of different geometries to small O_2 doses at a translational energy of the beam of $E_i = 0.39$ eV and at a crystal temperature $T = 100$ K. The angle of incidence was chosen normal to the crystal for Ag(100) and normal to the (110) step heights for the stepped surfaces. The two different sputtering temperatures, T_{sput}, correspond to different nanopatternings of the surface [6]. At low T_{sput} the surface is heavily damaged, while at $T_{sput} = 295$ K a checkerboard structure of square pits forms. The pits consist of a staircase of ordered (100) terraces and close-packed steps, with a high density of kinks at the corners.

Under the present dosing conditions only admolecules are observed on flat Ag(100), at least for small exposures. This result is manifested in the HREEL spectra by the loss feature

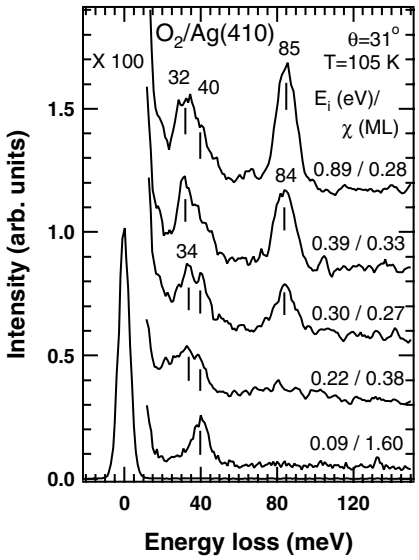

Figure 3. HREEL spectra for O_2 adsorption on Ag(410) at $T = 105$ K and different impact energies of the gas-phase molecules. The supersonic molecular beam hits the surface at $\theta = 31^\circ$, i.e. normally to the step heights. Only dissociative adsorption is observed at the lowest E_i as witnessed by the vibration at 40 meV. A different adatom species (loss at 34 meV) forms at slightly larger E_i. Also admolecules are populated for $E_I \geqslant 0.3$ eV.

at 81 meV [26], corresponding to the internal stretch motions of O_2 moieties, and by the absence of intensity in the frequency region of the O/Ag stretch, around 30–40 meV [27]. Two different O_2 species, vibrating at 79 and 84 meV, were reported in high-resolution experiments for Ag(110) [28] and Ag(100) [26] (the two contributions are not resolved in the spectrum reported in figure 2), and assigned to admolecules sitting, respectively, at hollow and at bridge sites (long bridges for Ag(110) and more probably short bridges for Ag(100)).

For damaged and stepped Ag surfaces, in contrast, loss of intensity is always present in the low-frequency region, indicating that non-thermal dissociation takes place. Molecular adsorption is totally suppressed for Ag(210) (uppermost spectrum of figure 2). A minimal terrace width is therefore necessary to stabilize the admolecules.

The vibrational frequencies of adatoms and admolecules are slightly different for the different structures. For Ag(410) the loss is composed of contributions, at 32 and 40 meV respectively, which are most probably present but not resolved, and also for the sputtered surfaces; only the 40 meV mode is observed, in contrast, for Ag(210). The lower frequency is close to the one observed for thermally dissociated adatoms on Ag(100) [22], while the higher one was reported for oxygen adatoms on Ag(110) [29]. The internal stretch frequency of O_2 reads 81 meV on flat and sputtered Ag(100) and 84 meV on Ag(410), implying that the molecules are in the peroxide state in all cases. On Ag(410) only the high-frequency moiety is therefore stable.

Figure 3 reports HREEL spectra recorded after dosing O_2 on Ag(410) with beams of different energy, $T = 105$ K, and $\theta = 31^\circ$ (molecules hitting normally to the step heights). At the lowest E_i the spectra are dominated by a loss at 40 meV and no intensity is present at higher frequency; only dissociative adsorption takes place therefore. The vibrational energy coincides with that of added-row reconstructed O/Ag(110) [29] and of O/Ag(210); see figure 2. When dosing at slightly higher E_i, the loss peak consists of two components, at 34 and 40 meV, indicating that the adatoms occupy two non-equivalent sites. As no intensity

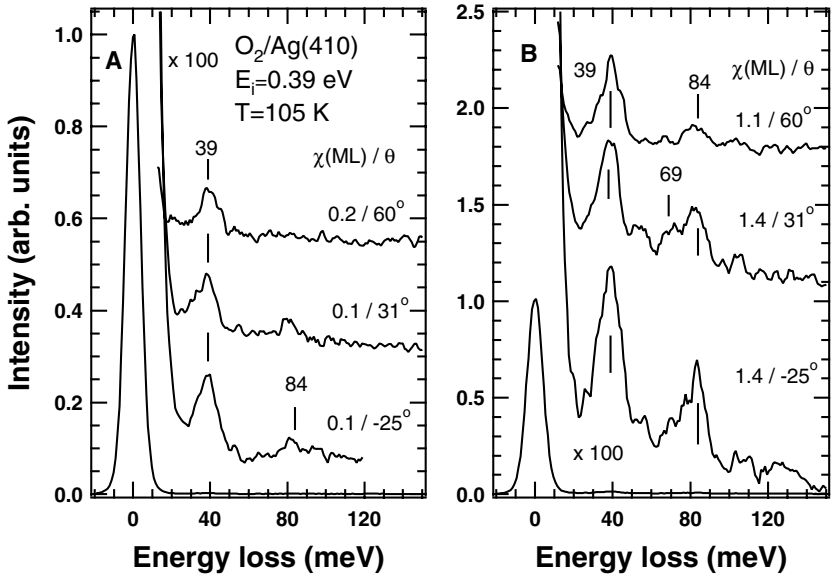

Figure 4. HREEL spectra recorded after dosing O_2 on Ag(410) at $T = 105$ K with $E_i = 0.39$ eV and parametric in the angle of incidence. Panel A: low-exposure limit; panel B: relatively large exposure. The final adsorption state is initially dissociative for all angles of incidence. Admolecules are eventually stabilized and are observed already at relatively low total coverage. The deactivation of the active site for dissociation occurs most probably through the action of nearby oxygen adatoms. The molecular adsorption site is reached more efficiently when the beam strikes normally to the step heights.

is present in the higher-frequency range, the final adsorption state is still only dissociative. At $E_i > 0.25$ eV a new loss arises at 84 meV; both adatoms and admolecules are therefore present. The molecule–surface stretch is at $\approx$30 meV for Ag(110) and Ag(100) [30,31]. At low coverage the intensity is rather weak for Ag(100) but not negligible for Ag(110). Comparing the spectra for $E_i = 0.22$ and 0.30 eV in figure 3, we conclude however that the O_2/Ag(410) stretch does not contribute significantly to the intensity in the low-frequency region, which is therefore still due to adatoms. From this experiment we conclude that molecular adsorption is globally activated also for Ag(410), but pathways leading to dissociation exist and have a small or vanishing adsorption barrier.

In figure 4 we show HREEL spectra recorded after dosing O_2 on Ag(410) with $E_i = 0.39$ eV, $T = 105$ K, and parametric in the angle of incidence. At small doses (panel A) dissociative adsorption dominates for all angles, while admolecules are present only when dosing either at $\theta = -25^\circ$ or normal to the step heights. The channel leading to stable molecular adsorption is therefore directional. After longer exposures (panel B) the population of both adatoms and admolecules has increased. At $\theta = 60^\circ$ the intensity of the loss at 84 meV is however still quite low. For the other angles the ratio of the two species has changed in favour of the admolecules. O_2 molecules impinging close to adatoms end up therefore in an undissociated state. A similar effect was reported for NO on Ni(100) [32].

The loss associated with the adatoms is at 39 meV for all angles. For $\theta = 31^\circ$ the result is in apparent contradiction with the spectrum at an intermediate exposure reported in figure 3. The loss at 34 meV is however expected to shift to higher frequencies with coverage because of the dipolar interaction and therefore not to be separable any longer from the loss at 40 meV.

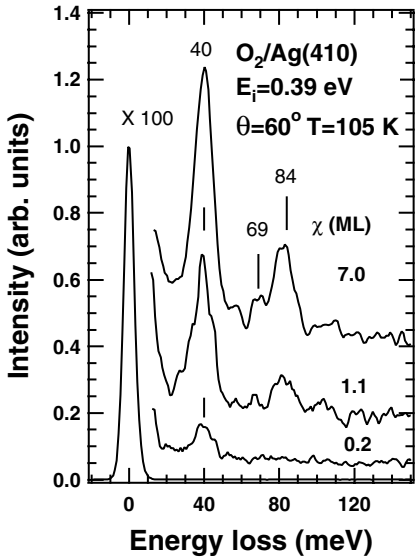

Figure 5. HREEL spectra recorded after exposing Ag(410) at $T = 105$ K to different doses of O_2 at $\theta = 60^\circ$ and $E_i = 0.39$ eV.

More interestingly, at the large exposure the internal O_2 vibration has a shoulder at 69 meV. As will be shown hereafter, such a peak persists also at temperatures at which only dissociative adsorption is stable. It is therefore most probably related to the frustrated translation of the oxygen adatoms, which becomes visible because of the reduced (410) symmetry.

In figure 5 the HREEL spectra, recorded after exposing the Ag(410) surface at $T = 105$ K to increasing O_2 doses, χ, are compared. The beam energy is $E_i = 0.39$ eV and the angle of incidence $\theta = 60^\circ$. Only dissociative adsorption is observed at the lowest χ while admolecules accumulate eventually. The phenomenon takes place, however, long before the intensity of the loss at 40 meV has reached saturation. We remark moreover that the shoulder at 69 meV develops also when dosing at this θ. Since the energy loss associated with the adatom stretch reads 40 meV independently of χ, this pathway populates mainly one adatom moiety.

The thermal evolution of the oxygen layer on Ag(410), after flashing the crystal to different crystal temperatures, is shown by the HREEL spectra of figure 6. In the experiment of panel A only adatoms are present; the loss at 40 meV is stable up to 240 K and shifts to 29 meV when flashing to 350 K. In the experiment of panel B non-dissociative adsorption has also occurred. The 40 meV loss remains stable up to 190 K and shifts to 34 meV when flashing to 300 K. The higher final frequency is due to the different annealing temperature. The shift from 34 to 30 meV when heating above RT takes place also for Ag(100). In that case it is associated with a change in the oxidation state of the adatoms, witnessed by the O 1s binding energy moving from 530.3 to 528.3 eV, and by a change in the adsorption site (from the grooves of the missing-row reconstruction below RT to fourfold hollow above RT) [27]. We notice, moreover, that while the 84 meV loss disappears above 155 K, the 69 meV loss persists up to 190 K. It is therefore connected with atomic oxygen species, in accord with our assignment to their frustrated translational motion.

When the exposure is performed at $T = 190$ K, as shown in figure 7, only adatoms form, and the stretch frequency reads 34 meV independently of E_i and exposure. Such frequency coincides both with the one observed after thermal dissociation in the low-coverage limit for flat

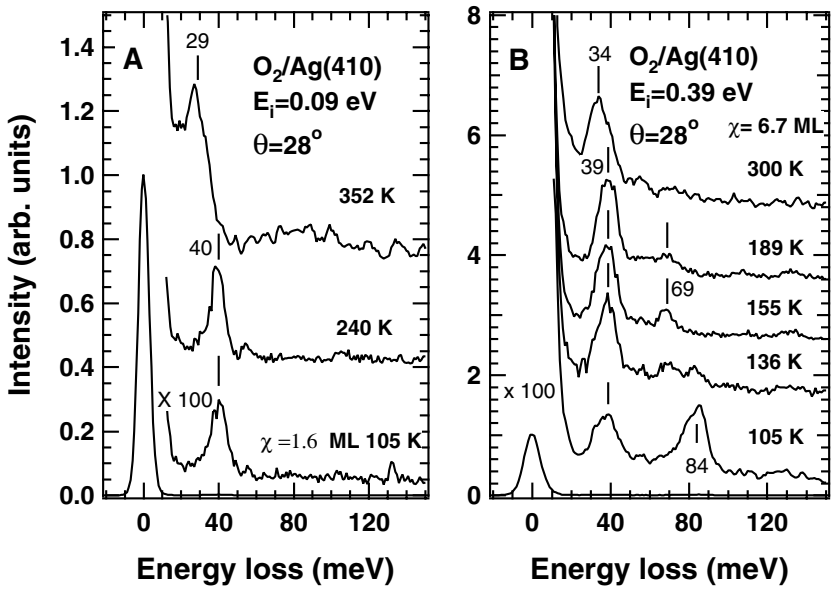

Figure 6. Thermal evolution of an O_2 layer after flashing the crystal to different crystal temperatures. Panel A: O_2 is dosed with $E_i = 0.09$ eV; panel B: $E_i = 0.39$ eV.

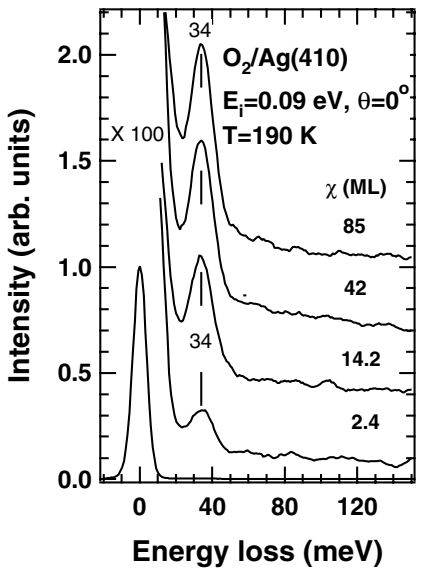

Figure 7. HREEL spectra recorded after exposing Ag(410) at $T = 190$ K to an O_2 beam with $E_i = 0.09$ eV at $\theta = 0°$. Only the dissociative adsorption site is occupied and the vibrational frequency coincides with that of O/Ag(100) at low coverage.

Ag(100) [31] and with the frequency observed for oxygen at Ag(100) surfaces nanostructured with square pits [7]. This result is apparently at variance with the spectra reported in figure 6, recorded after dosing at $T = 105$ K and eventually flashing the crystal to a given temperature, as the loss energy then remains stable at 40 meV up to 240 K. The different behaviour is due to the

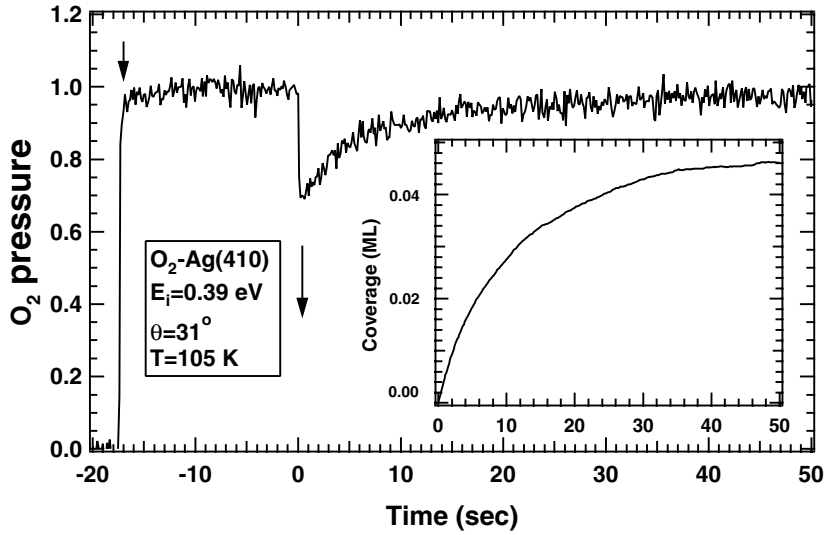

Figure 8. The normalized QMS trace for a retarded reflector adsorption experiment. The O_2 uptake obtained by integration of the sticking coefficient is reported in the inset.

longer annealing time of the experiments in figure 7 and to the fact that diffusion processes are coverage dependent, too. Reaching a certain coverage at $T = 105$ K and annealing is therefore not equivalent to reaching the same coverage when dosing at $T = 190$ K. Independently of the nature of the intermediate states, the final adsorption site is therefore the same as soon as the system is allowed to relax.

We suggest that both the 40 and the 34 meV modes correspond to oxygen atoms at the step edges. The different frequency could be determined either by the relaxation of the Ag atoms in Ag–O chains or by the separation of the oxygen adatoms at the steps. Since for high enough E_i the 34 meV state is observed at all dosing temperatures, when the dissociation event leading to this state takes place at low T, the translational energy must still be partly available and the molecular precursor must not have thermalized yet.

Let us now analyse the results of adsorption experiments performed with the retarded reflector method. The QMS trace for a typical KW experiment is shown in figure 8. At time $t = -18$ s the O_2 beam enters the main chamber and is intercepted by an inert shutter in front of the sample. The O_2 partial pressure is then determined by the beam flux and by the pumping speed of the chamber. When the shutter is removed, at time $t = 0$, the beam strikes the surface and the O_2 partial pressure decreases because of the additional pumping action of the surface. The relative pressure drop is the sticking coefficient, S. Upon saturating the oxygen layer, S decreases to zero. Integration of the $S(t)$ curve multiplied by the O_2 flux gives the surface coverage (Θ, in O_2 monolayers); see the inset of figure 8.

The initial drop in the QMS traces, S_0, corresponds to the interaction with the bare surface and is therefore particularly instructive. Its behaviour against E_i is reported in figure 9 for $\theta = 0^\circ$ (panel A) and for $\theta = -30^\circ$ and $+31^\circ$ (panel B). In panel A the results for Ag(410) are compared with those for the flat Ag(100) and Ag(110) surfaces and for sputtered Ag(100). Firstly, S_0 increases with E_i indicating that adsorption is also globally activated in the presence of defects. Secondly, at large E_i, S_0 is significantly smaller in the presence of defects than for flat surfaces and the values for Ag(410) coincide with those of the ordered pit structure obtained by bombarding Ag(100) at $T_{sput} = 325$ K. Thirdly, there is an anomalous behaviour

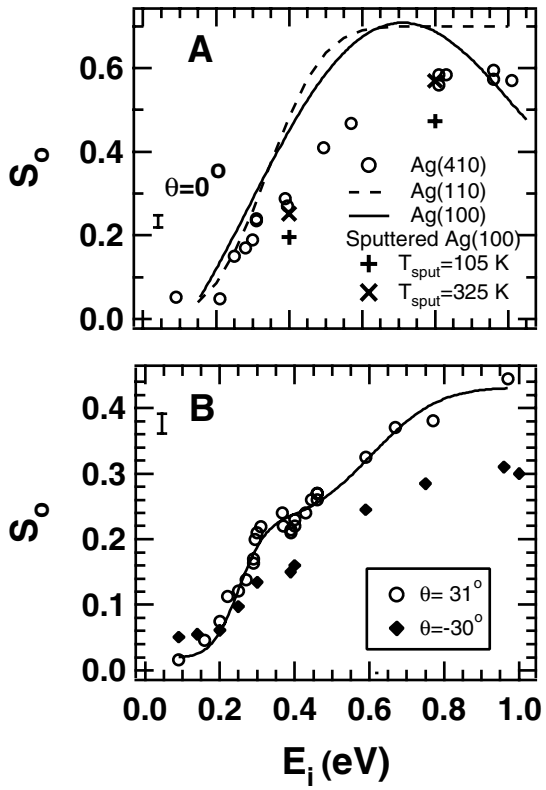

Figure 9. S_0-dependence versus E_i: panel A: comparison with flat Ag(110) and flat and sputtered Ag(100) at normal incidence; panel B: data recorded at $\theta = +31^\circ$ and -30°.

for $0.3 < E_i < 0.4$ eV where the slope of the $S_0(E_i)$ curve is smaller. This effect is larger when shooting O_2 normally to the step heights, as shown in figure 9, panel B.

To fit the curve for $\theta = 31^\circ$, two error functions (S-shaped curves) are needed, providing average barriers of 0.25 and 0.60 eV. The former barrier distribution is ascribed to the interaction of O_2 with steps, while the latter value is appropriate for the interaction with the terraces. Indeed on correcting for non-normal incidence with respect to the terraces, it reads 0.3 eV. Finally we remark that, at low E_i, S_0 is larger than for the flat surfaces, being still measurable for Ag(410) and much lower than the sensitivity of the KW method for Ag(100) and Ag(110). In this energy range S is therefore enhanced by a factor of $\approx$20 because of the opening of defect-related, non-activated adsorption channels.

The angular dependence of S_0 is reported in figure 10, parametric in E_i. At $E_i = 0.09$ eV $S_0(\theta)$ is nearly isotropic; at higher energies it is peaked along a direction which depends on E_i and moves towards the surface normal with increasing translational energy. We notice the following:

(i) For $E_i = 0.22$ eV, i.e. close to the first threshold of the $S_0(E_i)$ curve of figure 9, panel B, the maximum is nearly normal to the step heights. It corresponds therefore to the onset of molecular adsorption at steps.

(ii) Also, at the largest E_i the sticking probability is higher for molecules impinging with the parallel velocity component directed towards the ascending steps.

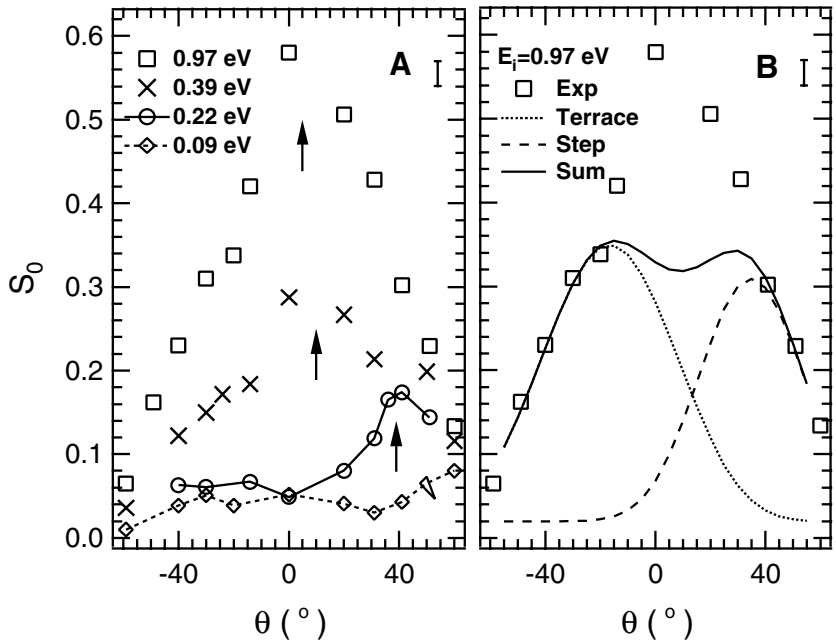

Figure 10. Panel A: S_0 versus θ, parametric in E_i. Panel B: a fit to the data recorded at $E_i = 0.97$ eV with the fitting functions reported in the text centred at angles corresponding to the normal to the terraces and to the step heights. A further contribution centred at $\theta = 0°$ is clearly needed to reproduce the data.

At $E_i = 0.97$ eV, molecules hitting at 45° against the terraces have a four-times-larger probability of sticking if they move a step up ($\theta = 31°$) than if they move a step down ($\theta = -59°$; the step heights are not exposed). Interestingly, the sticking probability for step-up motion is slightly larger than the one reported at 45° for flat Ag(100) ($S_0 = 0.42$ versus 0.35). Correcting for the relative weight of step heights and terraces at that angle, we obtain that S_0 is nearly unity at step heights. For a defected surface the O_2 sticking probability is thus enhanced at steps and strongly reduced at terraces with respect to Ag(100).

Supposing that step heights and terraces contribute additively to the total sticking probability, one could try to fit the $S_0(\theta)$ curve with a function of the form

$$S_0(\theta) = S_{0t} A_t(\theta) \cos^{n_t}(\theta + 14°) + S_{0s} A_s(\theta) \cos^{n_s}(\theta - 31°) + K \qquad (1)$$

where A_t and A_s are weight factors describing the relative projection at given angle of the area of terrace and step height nanofacets, K is a constant, and S_{0t} and S_{0s} are the sticking coefficients at terraces and step heights, respectively. In figure 10, panel B, we show however that no good fit can be achieved in this way. Fitting the data at large positive and negative angles we obtain sharply peaked distributions, as expected for activated adsorption ($S_{0t} = 0.4$, $n_t = 7.0$, and $S_{0s} = 0.8$, $n_s = 14$). However, S_{0s} is too large to be compatible with the value determined for $\theta = 31°$ [33] and the fit fails to reproduce the data at normal incidence for which another component is clearly needed. The stepped surface is therefore more complicated than the mere superposition of (100) and (110) nanofacets.

The temperature dependence of S_0 is reported in figure 11 for positive and negative angles, at which it has a similar value, and for different impact energies. Its behaviour is quite different to that for Ag(100), where it drops abruptly at $T = 170$ K [34], i.e. as soon as the desorption from the molecular well sets in. For Ag(410), S_0 decreases smoothly from $T = 105$ to 260 K

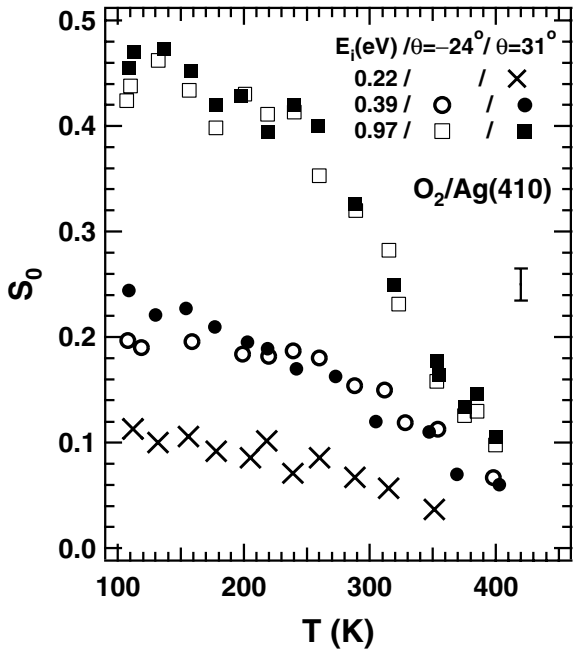

Figure 11. The temperature dependence of S_0, parametric in θ and in E_i. The shape of the curve is determined by the interplay between desorption and dissociation. The former occurs at all sites, while the latter takes place only at the step.

and more rapidly above that temperature. This behaviour, similar to that of O_2/Ag(110) [23], results from the competition between dissociation and desorption within the time constant of the vacuum system (0.3 s). The curves for Ag(410) and Ag(110) coincide up to 350 K, at which temperature the slope of $S_0(T)$ becomes steeper than for Ag(410). The difference is due the dissociation process, which occurs only at steps for Ag(410) and takes place at regular sites for Ag(110). When the lifetime in the chemisorbed state becomes shorter than the time needed to search for the defect, the dissociation probability for Ag(410) decreases therefore more rapidly than for Ag(110), where no searching is necessary.

Finally we notice that for $E_i = 0.97$ eV the $S_0(T)$ curve has a fine structure below 260 K, the derivative being zero for $200 < T < 250$ K. Such an effect is present at both angles of incidence and, although small, is outside the experimental error. This effect could be due to the presence of different desorption pathways connected to terrace and step sites.

The bottom trace in figure 11 corresponds to adsorption at $E_i = 0.22$ eV, a condition for which the final adsorption state is dissociative. S_0 decreases with T implying that dissociation is mediated by a molecular precursor. The same holds true also for $E_i = 0.09$ eV (not shown).

The dependence of S versus coverage and of coverage versus exposure time are reported in the upper panels of figure 12 for $\theta = 31^\circ$ and for different E_i. The maximum uptake, $\Theta_{\max}$, increases with kinetic energy, indicating that sites not available to the slow molecules can be accessed by the faster ones. This result is thus in agreement with our HREELS analysis, which shows that the access to the molecular adsorption site is activated. The so-determined value of $\Theta_{\max}$ is slightly lower than for Ag(110) and Ag(100). This coverage should not to be confused with the saturation one, which cannot be determined by KW measurements. Θ_{max} is anyway indicative of the relative availability of sites for the different dosing conditions.

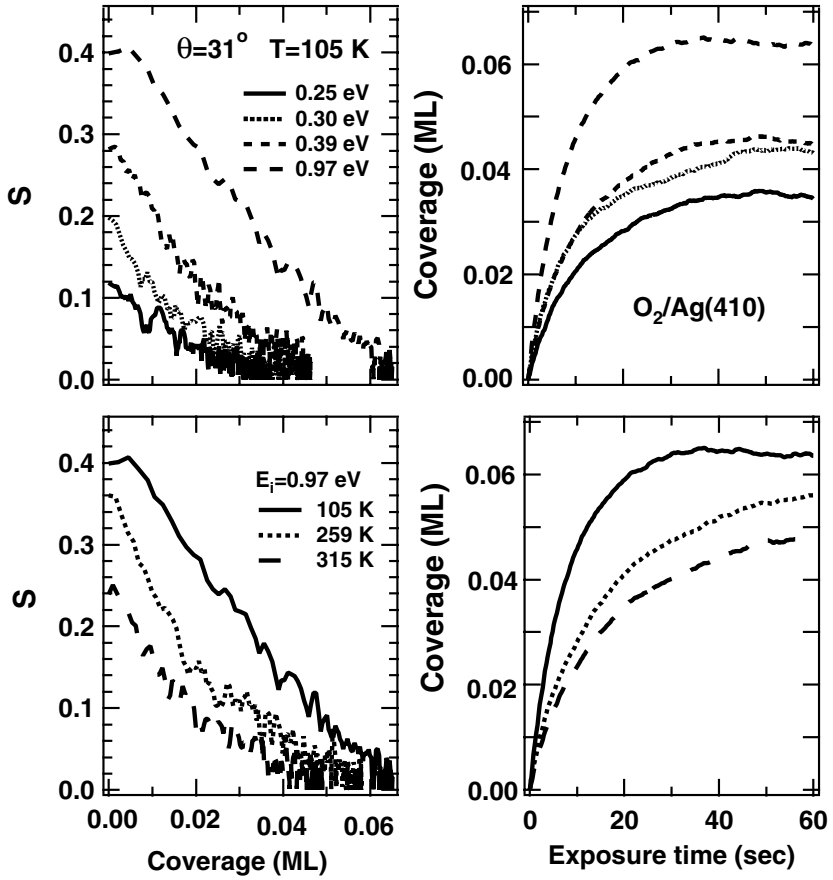

Figure 12. Coverage dependence of S (left panels) and total uptake curves (right panels) determined from the KW traces for $\theta = 31^{\circ}$: upper panels, versus E_i; lower panels, versus crystal temperature T.

A similar analysis is shown in the lower panels of figure 12 for traces recorded dosing with $E_i = 0.97$ eV at different surface temperatures, corresponding to the different adsorption states of the adsorbate. Θ_{max} is largest when admolecules are also stable ($T = 105$ K), it decreases when adsorption is entirely dissociative with the adatoms decorating the step edges (vibrational energy 34 meV, $T = 259$ K), and it is lowest when the oxygen adatoms move to the fourfold hollows (O/Ag vibration at 30 meV, $T = 315$ K).

4. Discussion

Our HREELS and KW data allow us to unambiguously identify the open steps with the active site for O_2 dissociation on otherwise inert Ag(100) surfaces. For Ag(210), where the terraces contain no complete (100) unit cell, the adsorption process indeed leads to the formation of adatoms only. When larger terraces are present, as is the case for Ag(410), adatoms and admolecules coexist. The HREEL spectra show that, when dosing at $T = 105$ K, dissociation is dominant at very low coverage and that the population of admolecules grows thereafter. We propose therefore that the oxygen adatoms play an active role in stabilizing the admolecules

by inhibiting dissociation in the neighbouring sites. At the lowest temperature, as long as the adsorbates are nearly immobile, inhibition of dissociation can thus occur already at low total coverage. A similar phenomenon was observed for NO/Ni(100), where lateral interactions between adatoms prevent NO dissociation and stabilize molecular adsorption [32].

At the lowest impact energies only dissociative adsorption is observed. This channel is non-activated but, since the sticking coefficient decreases with crystal temperature also at $E_i = 0.09$ eV, the adsorption process must be mediated by a molecular precursor. We propose that this pathway corresponds to gas-phase molecules hitting close to the step edge. The vibrational frequency of 40 meV suggests that the final chemisorption state consists of Ag–O chains at the step edge, similar to the added rows forming on Ag(110). This process takes place also on Ag(210).

Molecular adsorption occurs on Ag(410) only at higher E_i. When the gas-phase molecules impinge normally to the step heights, two barrier distributions are necessary to fit the energy dependence of the retarded reflector data. The former one has an average value $E_B = 0.25$ eV and it is thus lower than for flat Ag(100) or Ag(110), for which it reads 0.37 eV [13]. The higher one, in contrast, has an average value compatible with flat surfaces. The adsorption process occurs therefore, with increasing E_i, firstly at steps and eventually at terraces. The final non-dissociative adsorption state is however most probably the same, being characterized by only one value (84 meV) of the internal stretch vibration. On Ag(100) and Ag(110) this frequency corresponds to peroxide molecules at bridge sites, with the molecular axis parallel to the surface plane [26, 28]. Since the maximal coverage is lower than the step density, we believe that on Ag(410) the admolecules sit at the steps, too, the dissociation being inhibited by the presence of oxygen adatoms at neighbouring step sites. A similar observation was reported for H_2/Pd(210), where, in the presence of H adatoms, H_2 adsorption is stabilized at $T = 50$ K although atomic adsorption sites are still available [35, 36].

When dosing above $E_i = 0.22$ eV and $\theta = 31^\circ$, also adatoms characterized by the lower vibrational energy of 34 meV form. This loss is observed also when annealing the O moiety vibrating at 40 meV to $T = 190$ K or when dosing O_2 at that temperature. This frequency is moreover observed after thermal dissociation for Ag(100), but not on Ag(210) [37]. These adatoms may correspond either to oxygen in relaxed Ag–O chains or to oxygen at non-adjacent step sites. In the latter case however it should be possible to create such a configuration also for Ag(210), contrary to experimental evidence. Substrate relaxation should therefore take place only if the step is confined with a (100) terrace. Indeed an activation barrier must be overcome to reach this state. The required energy is supplied by the phonon bath when T is high enough, or by the translational energy of the gas-phase molecules when the substrate is immobile.

Finally, the global sticking probability in the presence of defects is smaller than for flat surfaces. Indeed our data coincide with the value found for checkerboard structure on Ag(100). The increased reactivity for molecular adsorption at the step edges must therefore be overcompensated by the reduced activity at terrace sites. This is indeed demonstrated directly by the low sticking coefficient found in experiments in which the beam hits the surface at such angles that the step heights are not exposed.

5. Conclusions

In conclusion, we have shown that open steps play a decisive role in the dynamics of the interaction of O_2 with Ag surfaces and that a stepped Ag(100) surface is more complicated than the superposition of (110) and (100) nanofacets.

We expect these phenomena to be quite general and important for catalytic reactions where either the adsorption of one of the reactants is strongly activated or dissociation is needed, with the result that the overall reaction rate is determined by adsorption at minority sites.

Acknowledgments

We acknowledge the financial support of the project COFIN 2001 of the Italian Ministry of Research (MURST) and scientific discussion with G Rovida and P Woodruff.

References

[1] Ertl G 2000 *Adv. Catal.* **45** 1
[2] Zambelli T, Wintterlin J, Trost J and Ertl G 1996 *Science* **273** 1688
[3] Hammer B 1999 *Phys. Rev. Lett.* **83** 3681
[4] Dahl S, Logadottir A, Egeberg R C, Larsen J H, Chorkendorff I, Tornqvist E and Norskov J K 1999 *Phys. Rev. Lett.* **83** 1814
[5] Mortensen H, Diekhoner L, Baurichter A, Jensen E and Luntz A C 2000 *J. Chem. Phys.* **113** 6882
[6] Costantini G, Buatier de Mongeot F, Rusponi S, Boragno C, Valbusa U, Vattuone L, Burghaus U, Savio L and Rocca M 2000 *J. Chem. Phys.* **112** 6840
[7] Vattuone L, Burghaus U, Savio L Rocca M, Costantini G, Buatier de Mongeot F, Rusponi S, Boragno C and Valbusa U 2001 *J. Chem. Phys.* **115** 3346
[8] Gee A T and Hayden B E 2000 *J. Chem. Phys.* **113** 10 333
[9] Brown W A, Kose R and King D A 1999 *Surf. Sci.* **440** 271
[10] Campbell C T and Paffett M 1984 *Surf. Sci.* **139** 396
[11] Van Santen R A and Kuipers H P C 1990 *Adv. Catal.* **35** 256
[12] Campbell C T 1985 *Surf. Sci.* **157** 43
[13] Rocca M 1996 *Phys. Scr.* **T66** 262
[14] Vattuone L, Rocca M, Boragno C and Valbusa U 1994 *J. Chem. Phys.* **101** 713
[15] Backx C, de Groot C P M and Biloen P 1981 *Surf. Sci.* **104** 300
[16] Buatier de Mongeot F, Rocca M and Valbusa U 1996 *Surf. Sci.* **363** 68
[17] Campbell C T 1986 *Surf. Sci.* **173** L641
[18] Raukema A and Kleyn A W 1995 *Phys. Rev. Lett.* **74** 4333
[19] Raukema A, Butler D A, Box F M A and Kleyn A W 1996 *Surf. Sci.* **347** 151
[20] Buatier de Mongeot F, Valbusa U and Rocca M 1995 *Surf. Sci.* **339** 291
[21] Rocca M, Cemic F, Buatier de Mongeot F, Valbusa U, Lacombe S and Jacobi K 1997 *Surf. Sci.* **373** 125
[22] Buatier de Mongeot F, Cupolillo A, Valbusa U and Rocca M 1999 *Chem. Phys. Lett.* **302** 302
[23] Savio L, Vattuone L and Rocca M 2001 *Phys. Rev. Lett.* **87** 276101
[24] Rocca M, Valbusa U, Gussoni A, Maloberti G and Racca L 1991 *Rev. Sci. Instrum.* **62** 2171
[25] King D A and Wells M G 1972 *Surf. Sci.* **29** 454
[26] Vattuone L, Gambardella P, Valbusa U and Rocca M 1997 *Surf. Sci.* **377–9** 671
[27] Rocca M *et al* 2000 *Phys. Rev.* B **61** 213
[28] Bartolucci F, Franchy R, Barnard J and Palmer R E 1998 *Phys. Rev. Lett.* **80** 5224
[29] Vattuone L, Rocca M and Valbusa U 1996 *Surf. Sci.* **369** 336
[30] Rocca M, Vattuone L, Boragno C and Valbusa U 1993 *J. Electron Spectrosc. Relat. Phenom.* **64/65** 577
[31] Buatier de Mongeot F, Cupolillo A, Valbusa U and Rocca M 1997 *J. Chem. Phys.* **106** 6297
[32] Vattuone L, Yeo Y Y and King D A 1996 *Catal. Lett.* **41** 919
[33] Rocca M, Savio L and Vattuone L 2002 *Surf. Sci.*
[34] Buatier de Mongeot F, Rocca M and Valbusa U 1997 *Surf. Sci.* **377/379** 691
[35] Schmidt P K, Christmann K, Kresse G, Hafner J and Lischka M Gross A 2001 *Phys. Rev. Lett.* **87** 096103
[36] Lischka M and Gross A 2002 *Phys. Rev.* B **65** 075420
[37] Vattuone L, Savio L and Rocca M 2002 at press